The Iranian Journal of Mechanical Engineering Transactions of ISME
Journal homepage: https://jmee.isme.ir/
Vol. 25, No. 1, 2024, pp. 65-88

Research Paper

DOI: https://doi.org/10.30506/jmee.2024.2015439.1331

A Novel Switching Control Scheme for Rehabilitation of the Lower Limbs of a Human Body

Farhad Rezvani*
Ph.D. Candidate

Hamidreza Mohammadi Daniali†
Professor

Khodabakhsh Javanshir‡
Associate Professor

This paper presents a novel algorithm for the control of a 2D rehabilitation cable robot for the lower limb, addressing the dynamic model of the lower limb movements in the sagittal plane. Considering the nonlinear dynamic interactions between subsystems, the proposed control algorithm utilizes impedance control for torque and position control in knee and hip during passive and active-assistive rehabilitation modes. A switching algorithm is implemented for the cable forces. The system features two connected cables for each limb, with one active cable at any given time, positioned at the front and back, aiming to enhance patient comfort and perception of rehabilitation. The simulation results indicate a short run-time and negligible tracking error in torque and position for the limb.

Keywords: Cable robot, Sagittal plane, Impedance control, Rehabilitation mode, Switching algorithm

1 Introduction

Motor rehabilitation is a crucial process that aids patients in recovering their motion ability after experiencing motion disability. Physiotherapists usually encourage patients to perform desired motion patterns within a specific period. In recent decades, robotic systems have been developed to assist in this process, reducing the physiotherapist's effort and the cost [1]. These systems can be divided into two groups; namely, exoskeleton and end-effector. The use of a second robotic system that does not require precise geometric design and can be used for any patient has been noted.

*Ph.D. Candidate, Department of Mechanical Engineering, Babol Noshirvani University of Technology, Babol, Iran, f.rezvani@stu.nit.ac.ir
†Corresponding Author, Professor, Department of Mechanical Engineering, Babol Noshirvani University of Technology, Babol, Iran, mohammadi@nit.ac.ir
‡Associate Professor, Physical Therapy Department, Faculty of Rehabilitation, Babol University of Medical Sciences, Babol, Iran, kjavanshir@yahoo.com

Received: 2023/11/21, Revised: 2024/03/11, Accepted: 2024/04/13

Cable robots are highly flexible, can change configurations, have proper inertia, low cost and simple maintenance. The first studies on rehabilitation cable robots were conducted by Rossi [2]. Sophia-3 [3] was the first adaptive cable robot for hand rehabilitation, and upon increasing the cables and introducin0g redundancy, CALT was designed for lower limb rehabilitation of spinal cord injury patients [4]. In [5], A model was also developed to estimate the active and passive joint moments of the ankle in three anatomical axes.

It is interesting to see the different approaches that have been taken in studying cable robots. Some researchers have calculated the robot workspace singularity and optimized it using particle swarm optimization [6], while others have added springs between the base and end-effector to modulate the workspace [7]. Moreover, in [8] the actuators positions of the robot has been optimized based on the minimum sum of cable tensions. It is clear that there are multiple factors to consider when working with cable robots, and it is important to take a comprehensive approach to optimization.

Rehabilitation robots can be categorized into three groups; namely, passive, active, and interactive. While the passive one is lighter, safer, cheaper, and easier to use, it has the drawback of relying solely on gravity force to help patients. On the other hand, active robots can control interaction forces and measure active forces, range of motion, and muscle spasticity precisely [9]. Interactive robots have expert control methods that react to patient effort based on feedback of force and position signals. To the best our knowledge position and force control has not been studied, simultaneously.

The study discussed in [10] presented a strategy for evaluating the interaction between patients and rehabilitation robots. A optimization method was exploited in [11] to design a robot for hand assistance and track the trajectory of fingers. Impedance/admittance controllers are widely used in rehabilitation applications because they are compliant and flexible, as noted in [12]. For instance, in [13], a control scheme was designed for the ARBOT ankle rehabilitation robot, and the control algorithm was selected based on the rehabilitation protocol. The interaction between the patient and the robot was also considered, with admittance control used for patient-active exercises and position control employed for patient-passive exercises. In [14], an ankle rehabilitation robot was introduced that also uses impedance control, with serial elastic actuation enabling plantar flexion and dorsiflexion motion in passive, fixed, and resistive modes. Moreover, ROMRES is a robot used for upper and lower limb rehabilitation, utilizing rule-based control and adapting to patient behavior. The robot can facilitate passive, active-assisted, and exercises for spasticity. Impedance controllers are used to facilitate patient-robot interaction in these cases [15].

Many people studied in the field of developing control methods to improve the gait rehabilitation of the patient [16-20]. A novel cable-driven lower limb rehabilitation robot (CDLLRR) with bilateral control, enhancing safety and adaptability in patient-therapist interaction. Detailed design and an improved PD controller (IPDAM) are introduced, validated through simulation experiments, affirming their efficacy in revolutionizing lower limb rehabilitation robotics in [21]. A cable-driven lower-limb rehab robot for bedridden patients. Using flexible cables, it actively drives hip and knee motions at the bedside. A human–cable coupling controller adjusts the cable forces based on joint impedance, enhancing stability. Experiments on five participants showed significant improvements in joint flexibility and stability [22]. There have been various studies conducted on the use of impedance control in robotics for rehabilitation purposes. One study proposed a method for designing impedance control for an upper limb rehabilitation robot, which varied the damping value according to the target position and tracking error [23]. Another study considered human uncertainty in the design of an impedance-based control approach to improve robot-assisted training [24]. This study used repetitive exercises to allow the user to adopt the impedance parameters according to their individual needs. In yet another study, muscular

effort distribution was measured to determine the participation of each muscle in training activity [25]. Advanced exercise protocols were created using impedance control, and users were asked to follow the robot's path against resistance. An adaptive impedance control law was developed for a parallel robot designed for ankle rehabilitation [26]. In [27] was focused on a lower limb robot and using a hybrid sliding mode impedance control, the robot was studied and optimized by Harmony Search Algorithm.
Finally, impedance control was used to study the resistive mode of rehabilitation in a mechanism in study [28].
Despite extensive research on the implementation of cable robots and control algorithms in lower limb rehabilitation, there remain unresolved issues. This study focuses on a 2-DOF cable robot with four cables, two connected to the leg and two connected to the shank, as depicted in Figure (1). Each limb has two connected cables, one at the front and one at the back, with only one cable active at any given time. This design prioritizes enhancing patient comfort and rehabilitation perception, aiming to improve synergy throughout the rehabilitation process. The study introduces a novel suboptimal switch control scheme using the impedance control method. This scheme allows dynamic switching between the two connected cables of each limb, facilitating the implementation of active-assistive and passive modes. Moreover, the study proposes a practical methodology for estimating applied torques to the lower limb induced by the patient's body. Importantly, the suboptimization algorithm is introduced to address some challenges associated with real-time control algorithms in the context of this rehabilitation approach.
This paper is divided into six sections. The dynamics of the cable robot and the lower limbs are presented in Section (2). The rehabilitation is categorized into three modes, each of which is described in Section (3). A new control algorithm is created to perform two of those modes in Section (4). The simulation of the control scheme is presented and the results are displayed in Section (5). Finally, the conclusion of the paper is presented in Section (6).

2 Dynamic modeling

In this section, dynamic modeling of the lower limb is presented.

2.1 Dynamic modeling of the lower limb

Figure (1) demonstrates the geometric parameters of the lower limb and some applied forces and torques, in which m_1 and m_2 are masses of the thigh and shank, respectively. Therefore, the applied gravitational forces are $m_1 g$ and$m_2 g$, respectively. Two linear torsional springs with stiffness K_1 and K_2 are attached to the hip and the knee joints, as well. Moreover, two linear torsional dampers with constants of C_1 and C_2 are attached. The applied torques to the joints due to the body are given by τ_1 and τ_2.
A cable robot with four cables and two degrees of freedom (DOF) is attached to the leg, as illustrated in Figure (2). The cables are attached to the leg with four cuffs.
The distance between the attached point of the cables to the leg and the central axis of the corresponding limb are given by w_i $(1, 2, 3, 4)$. They have positive value for the cables that are in the back of the thigh and the shank, while. For the cables in the front of the thigh and the shank they have negative value.
For the purpose of dynamic motion modeling, the lower limbs (thigh and shank) have been modeled as a two-degree-of-freedom pendulum, with the hip joint serving as its support. So, Lagrangian method is used here to derive the dynamic equation.
Firstly, the horizontal and vertical components of position of hip and knee center of mass are obtained as below:

$$\begin{cases} x_1 = c_1 \cos\theta_1 \\ y_1 = c_1 \sin\theta_1 \end{cases} \quad (1)$$

$$\begin{cases} x_2 = l_1 \cos\theta_1 + c_2 \cos(\theta_1 + \theta_2) \\ y_2 = l_1 \sin\theta_1 + c_2 \sin(\theta_1 + \theta_2) \end{cases} \quad (2)$$

Where θ_1 and θ_2 are generalized coordinates.
Therefore, the kinetic and potential energy of the robot system are given as:

$$K.E. = \frac{1}{2} m_1 (\dot{x}_1^2 + \dot{y}_1^2) + \frac{1}{2} m_2 (\dot{x}_2^2 + \dot{y}_2^2) + \frac{1}{2} m_1 R_1^2 \dot{\theta}_1^2 + \frac{1}{2} m_2 R_2^2 (\dot{\theta}_1 + \dot{\theta}_2)^2 \quad (3)$$

$$P.E. = -m_1 g x_1 - m_2 g x_2 + \frac{1}{2} K_1 \theta_1^2 + \frac{1}{2} K_2 \theta_2^2 \quad (4)$$

The virtual work of generalized forces includes: the virtual work of cables forces (δW_F), the virtual work of the applied torques to joints due to patient effort (δW_{τ_p}) and the virtual work of the torque due to torsional dampers (δW_C).

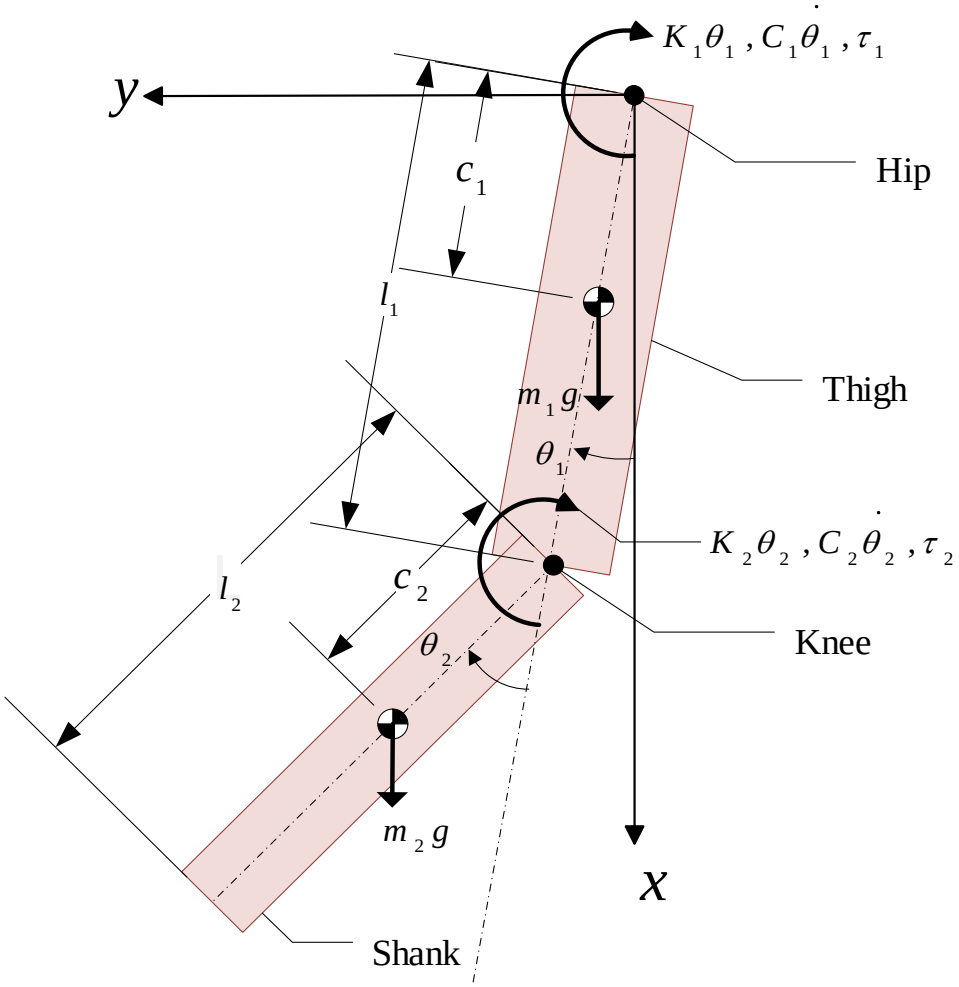

Figure 1 Schematic of the lower limb and corresponding parameters

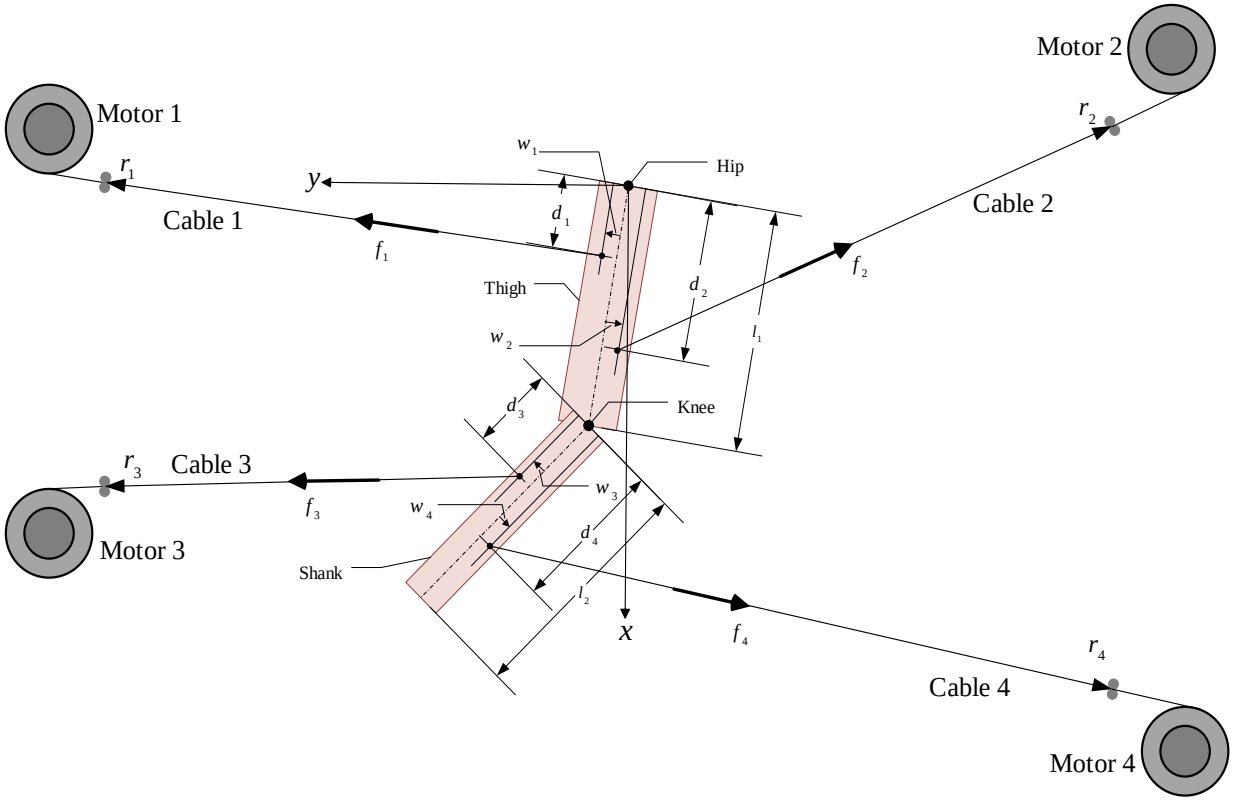

Figure 2 Schematic of the cable robot which is attached to the lower limb

Where δW, δW_τ and δW_C is given by the following equations in order to their physical concept:

$$\begin{cases} \delta W_F = -\sum_{i=1}^{4} \mathbf{F}_i \, \delta \mathbf{r}_i \\ \delta W_\tau = \sum_{j=1}^{2} \boldsymbol{\tau}_i \, \delta \boldsymbol{\theta}_j \qquad j = 1,2 \\ \delta W_C = -\sum_{ij=1}^{2} C_j \, \dot{\boldsymbol{\theta}}_j \delta \boldsymbol{\theta}_j \end{cases} \tag{5}$$

So, the resultant of the above virtual works is obtained as following:

$$\delta W = \delta W_F + \delta W_\tau + \delta W_C \tag{6}$$

In order to determination of the system motion equation in matrix form the vectors of joints angles, cables forces, internal torques and torques of gravity are introduced as following:

$$\begin{cases} \boldsymbol{\theta} = [\theta_1 \quad \theta_2]^T \\ \mathbf{f} = [f_1 \quad f_2 \quad f_3 \quad f_4]^T \\ \boldsymbol{\tau} = [\tau_1 \quad \tau_2]^T \\ \mathbf{g} = \begin{bmatrix} m_1 g c_1 \sin\theta_1 + m_2 g l_1 \sin\theta_1 + m_2 g c_2 \sin(\theta_1 + \theta_2) \\ m_2 g c_2 \sin(\theta_1 + \theta_2) \end{bmatrix} \end{cases} \tag{7}$$

Also, matrices of inertia, damping, stiffness and Jacobian of the cable forces to joints torque are expressed as:

$$\mathbf{M} = \begin{bmatrix} M_3 + (m_1 c_1^2 + m_2 l_1^2 + m_1 R_1^2) + m_2 c_2 l_1 \cos\theta_2 & M_3 + m_2 c_2 l_1 \cos\theta_2 \\ M_3 + m_2 c_2 l_1 \cos\theta_2 & M_3 \end{bmatrix} \tag{8}$$

$$\mathbf{C} = \mathbf{C}' + \mathbf{C}'' \tag{9}$$

$$\boldsymbol{K} = diag([K_1 \quad K_2]) \tag{10}$$

$$\mathbf{B} = \begin{bmatrix} B_{11} & B_{12} & B_{13} & B_{14} \\ B_{21} & B_{22} & B_{23} & B_{24} \end{bmatrix} \tag{11}$$

in which

$$\begin{cases} M_3 = m_2(c_2^2 + R_2^2) \\ \mathbf{C}' = \begin{bmatrix} -\mathbf{2} m_2 c_2 l_1 \dot{\theta}_2 \sin\theta_2 & -m_2 c_2 l_1 \dot{\theta}_2 \sin\theta_2 \\ m_2 c_2 l_1 \dot{\theta}_1 \sin\theta_2 & \mathbf{0} \end{bmatrix} \\ \mathbf{C}'' = diag([C_1 \quad C_2]) \end{cases} \tag{12}$$

$$B_{ij} = \left(\left(\frac{\partial \mathbf{r}_i}{\partial \theta_j} . \hat{\mathbf{i}} \right) r_{ix} + \left(\frac{\partial \mathbf{r}_i}{\partial \theta_j} . \hat{\mathbf{j}} \right) r_{iy} \right) \Big/ |\mathbf{r}_i| \tag{13}$$

also, R_1 and R_2 are the gyration radii of thigh and shank, respectively.
Therefore, matrix form of motion equation is given as following:

$$\mathbf{M}\ddot{\boldsymbol{\theta}} + \mathbf{C}\dot{\boldsymbol{\theta}} + \mathbf{K}\boldsymbol{\theta} + \mathbf{G} = \mathbf{B}\mathbf{f} + \boldsymbol{\tau} \tag{14}$$

2.2 Discretization of dynamic equations

The governing Equation (14) is nonlinear, obviously. Hence, they are solved here numerically. Therefore, they are discretized firstly, in which the angular acceleration vector is approximated as:

$$\dot{\boldsymbol{\theta}}(k) \simeq \big(\boldsymbol{\theta}(k+1) - \boldsymbol{\theta}(k)\big)/T \qquad k = 0,1,2,3,\ldots \tag{15}$$

in which T is sampling time.

2.3 Torques estimation

In Equation (14) the components of $\boldsymbol{\tau}$ should be measured at any time. Since, measuring of these are impossible or very difficult and their estimated values $\hat{\boldsymbol{\tau}}$ are used here. In order to estimate$\hat{\boldsymbol{\tau}}$, a torque meter is placed at the hip and knee joint. These torque meters measure the applied net torque ($\boldsymbol{\tau}_{net}$) to these joints. Therefore, Equation (14) can be rewrite as:

$$\mathbf{M}\ddot{\boldsymbol{\theta}} + \mathbf{C}'\dot{\boldsymbol{\theta}} = \boldsymbol{\tau}_{net} \tag{16}$$

Where

$$\boldsymbol{\tau}_{net} = -\mathbf{C}''\dot{\boldsymbol{\theta}} - \mathbf{K}\boldsymbol{\theta} - \mathbf{g} + \mathbf{B}\mathbf{f} + \boldsymbol{\tau} \tag{17}$$

The left side of Equation (16) is the inertia torque applied to the joints that is not measured by the torque meters, while the right side explain the static and semi-static torques that torque meters measure. Considering the generalized coordinates, the first and second rows of Equation (17) are the applied torques to the hip and the knee joints, respectively.
Because of the delay of measuring instruments and processors, the measured values of the toques are not applicable in real time. Therefore, at each time step, the measured values of the prior step time are used as the estimated values. Considering Equation (17), the net torques in the discretized domain at the prior step time are calculated and $\hat{\tau}$ is obtained as:

$$\hat{\boldsymbol{\tau}}(k) = \boldsymbol{\tau}_{\boldsymbol{net}}(k-1) + \mathbf{C}''\dot{\boldsymbol{\theta}}(k-1) + \mathbf{K}\boldsymbol{\theta}(k-1) + \mathbf{g}(k-1) - \mathbf{B}(k-1)\mathbf{f}(k-1) \tag{18}$$

3 Rehabilitation modes

There are three different strategies for mobility impairment treatment:
1) Passive mode in which the robot moves leg in a predefined path.
2) Active-assistive mode in which the patient moves his/her leg in a predefined path with the assistance of the robot.
3) Active-resistive mode in which the patient moves his/her leg in the opposite direction of the force that the robot imposes.

In this research, we study the modes 1 and 2 in a model of human leg.
Passive mode: at the early stage of rehabilitation, the patient suffers from injuries that lead to inability to move his/her hip and knee joints, so he/she is unable to apply the required torques to his/her joints. Therefore, it is needed to exert external torques to the patient for moving retrieval. The torques are exerted to the joints by cables which attached to the hip and the shank in a predesigned scenario. Therefore, it is needed to define a control algorithm to minimize angular position error of the patient joint related to a predesigned position. Therefore, the predesigned position is called by desired position which includes angle, angular velocity and angular acceleration of the patient joints and represents as $\boldsymbol{\theta}_d$, $\dot{\boldsymbol{\theta}}_d$ and $\ddot{\boldsymbol{\theta}}_d$, respectively. In order to design a control algorithm, angle error is defined as:

$$\tilde{\boldsymbol{\theta}}_{\boldsymbol{d}}(k) = \boldsymbol{\theta}_{\boldsymbol{d}}(k) - \boldsymbol{\theta}_{\boldsymbol{d}}(k) \tag{19}$$

in which,

$$\dot{\boldsymbol{\theta}}_{\boldsymbol{d}}(k) = \big(\boldsymbol{\theta}_{\boldsymbol{d}}(k+1) - \boldsymbol{\theta}_{\boldsymbol{d}}(k)\big)/T \qquad k = 1, 2, 3, \ldots \tag{20}$$

Thus, the dynamic error equations are formulated employing impedance control theory as [29]:

$$\mathbf{M}_{\boldsymbol{d}}\ddot{\tilde{\boldsymbol{\theta}}}(k) + \mathbf{C}_{\boldsymbol{d}}\dot{\tilde{\boldsymbol{\theta}}}(k) + \mathbf{K}_{\boldsymbol{d}}\tilde{\boldsymbol{\theta}}(k) = \mathbf{0} \tag{21}$$

Where, $\mathbf{M}_{\boldsymbol{d}}$, $\mathbf{C}_{\boldsymbol{d}}$ and $\mathbf{K}_{\boldsymbol{d}}$ are positive definite square matrixes. So that Equation (21) is asymptotically stable.
Active-assistive mode: after the first stage, the patient is capable of exerting some torques to the hip and the knee joints, but it is needed to increase the range of motion of the joints.

Indeed, at this stage, the patient does not have enough ability to exert the required torques to the joints. Hence, in order to do a predesigned motion completely, it is needed to help him/her. Therefore, the patient is asked to make an effort to perform these motions. Similar to the passive mode, a control algorithm is needed to minimize the angular position errors of the patient joints related to the predesigned positions. Therefore, error dynamic is obtained as Equation (21). Another difference of this mode from the passive mode is that in the active-assistive mode, the patient applies some torques to his/her joints, so $\boldsymbol{\tau}$ is not zero and according to Equation (18) must be estimated. Also, the error dynamic is described as Equation (21) for this mode.

4 Design of control algorithm

In this section, a control algorithm is designed such that covers the both modes of rehabilitation. So, control laws would maintain the Equation (21).
In order to select of appropriate values of, $\mathbf{M}_{\boldsymbol{d}}$, $\mathbf{C}_{\boldsymbol{d}}$ and $\mathbf{K}_{\boldsymbol{d}}$, Equation (21) is re-written as:

$$\mathbf{M}_{\boldsymbol{d}}^{*}\ddot{\tilde{\boldsymbol{\theta}}}(k+1)+\mathbf{C}_{\boldsymbol{d}}^{*}\dot{\tilde{\boldsymbol{\theta}}}(k)+\mathbf{K}_{\boldsymbol{d}}^{*}\tilde{\boldsymbol{\theta}}(k-1)=\mathbf{0} \tag{22}$$

where,

$$\begin{cases}\mathbf{M}_{\boldsymbol{d}}^{*}=\mathbf{M}_{\boldsymbol{d}}/T^{2}\\ \mathbf{C}_{\boldsymbol{d}}^{*}=-2\mathbf{M}_{\boldsymbol{d}}/T^{2}+\mathbf{C}_{\boldsymbol{d}}/T\\ \mathbf{K}_{\boldsymbol{d}}^{*}=\mathbf{M}_{\boldsymbol{d}}/T^{2}-\mathbf{C}_{\boldsymbol{d}}/T+\mathbf{K}_{\boldsymbol{d}}\end{cases} \tag{23}$$

The values of $\mathbf{M}_{\boldsymbol{d}}$, $\mathbf{C}_{\boldsymbol{d}}$ and $\mathbf{K}_{\boldsymbol{d}}$ should be selected such that $\tilde{\boldsymbol{\theta}}(k-1)$, $\dot{\tilde{\boldsymbol{\theta}}}(k-1)$ and $\ddot{\tilde{\boldsymbol{\theta}}}(k-1)$ are converge to zero uniformly and at a reasonable rate. For this purpose, the following conditions must be met:

a) $\mathbf{M}_{\boldsymbol{d}}$ should be positive definite.
b) System dynamics of Equation (22) should be asymptotically stable at a reasonable rate.
c) System behavior of Equation (22) should be non-oscillating.

To satisfy condition b, it is sufficient that all of the eigenvalues of the following matrix should be inside the unit circle.

$$\mathbf{A}_{d}=\begin{bmatrix}\mathbf{0} & \mathbf{I}\\ -(\mathbf{M}_{\boldsymbol{d}}^{*})^{-1}\mathbf{K}_{\boldsymbol{d}}^{*} & (\mathbf{M}_{\boldsymbol{d}}^{*})^{-1}\mathbf{C}_{\boldsymbol{d}}^{*}\end{bmatrix} \tag{24}$$

Also, to satisfy condition c, it is sufficient that all of the eigenvalues of matrix (24) must be real and positive.
Considering Equations (14), (19), (21), (22) and (23), to satisfy the above conditions, the values of f_1 to f_4 should be determined at any time practically. On the other hand, these values should be considered some practical considerations. These considerations can be expressed as following constraints:

a) Since the cables cannot exert compressive force, the values of the cables forces should be positive.
b) Since the actuators functional capacity is limited, the values of forces should not exceed their maximum value, namely, $\mathbf{f}_{\max}$.
c) Since the actuators functional capacity is limited for changing the magnitude of any force, the magnitude of change in each force should not be greater than a predefined allowed value; namely, $\Delta\mathbf{f}_{\max}$.

d) In order to have a permanent pre-tension in the cables, the values of forces should not be less than a predefined allowed value; namely, $\mathbf{f}_{\min}$.

The values of $\mathbf{f}_{\max}$, $\Delta\mathbf{f}_{\max}$ and $\mathbf{f}_{\min}$ are the force capacity of the actuators, the allowable changes in value of the cable forces at each time step and the value of the required pre-tension of the cables applied by actuators, respectively.

In order to design the control algorithm, Equation (22) is rewritten as following:

$$\mathbf{J}(k)\mathbf{f}(k) = \mathbf{h}'(k) + \mathbf{h}''(k) \tag{25}$$

where,

$$\begin{cases} \mathbf{H}'(k) = \mathbf{M_d}\ddot{\boldsymbol{\theta}}_{\boldsymbol{d}} + \mathbf{C_d}\dot{\tilde{\boldsymbol{\theta}}}(k) + \mathbf{K_d}\tilde{\boldsymbol{\theta}}(k) \\ \mathbf{H}''(k) = \mathbf{M_d}\mathbf{M}^{-1}(k)\left[\mathbf{C}\dot{\boldsymbol{\theta}} + \mathbf{K}\boldsymbol{\theta} - \hat{\boldsymbol{\tau}}(k)\right] \\ \mathbf{J}(k) = \mathbf{M_d}\mathbf{M}^{-1}(k)\mathbf{B}(k) \end{cases} \tag{26}$$

In order to determine the values of the forces, according to practical consideration, a system of equations with two equations and four unknowns (f_1 to f_4) should be solved. One of the conventional approaches to solving these cases is selecting the optimum solution in order to minimize a predefined target function. According to the nature of the present problem with expressed constraints, solving this problem leads to some iterative methods. Implementation of these methods using conventional computer software and hardware, is challenged by the real time in control algorithm. Therefore, to solve the present problem, a sub-optimization algorithm is proposed. According to the nature of the problem, most of the time the torques and the forces of cables (1) and (2) act in the opposite direction. It is the same in the case of cables (3) and (4). Therefore, the corresponding control command acts such that the actuators act on just two cables at any time. These cables are called active cables, while others are called inactive cables. Also, corresponding forces of these torques are called active forces ($\mathbf{f}_A$) and inactive forces ($\mathbf{f}_I$), respectively. So, there are four different cases of active pair cables, as follows:

Case (1): cables (1) and (3) are active.
Case (2): cables (1) and (4) are active.
Case (3): cables (2) and (3) are active.
Case (4): cables (2) and (4) are active.

Hence, at any time, active and inactive forces apply to the lower limb via active and inactive cables, respectively. This idea would decrease the control effort. Because the opposite cables do not neutralize each other's effects. On the hands, the patient senses the effect of just one cable on each of his/her limbs. It leads to the patient having a better perception of the rehabilitation and being more comfortable. Anyway, according to the magnitude and direction of the torques of applied forces to the joints, the controller should select the appropriate case at any time and calculate the values of the active forces. So, the desired control algorithm is presented as follows:

Step (1): for cases (1) to (4), according to Equation (25), active forces are obtained as follows and shown by $\mathbf{f}_{1A}$, $\mathbf{f}_{2A}$, $\mathbf{f}_{3A}$ and $\mathbf{f}_{4A}$, respectively:

$$\mathbf{f}_{jA}(k) = \mathbf{J}_{jA}^{-1}(k)\left(\mathbf{h}(k) - \mathbf{J}_{jI}(k)\mathbf{f}_{jI}\right) \qquad j = 1, 2, 3, 4 \tag{27}$$

where $\mathbf{J}_{jA}$ and $\mathbf{J}_{jI}$ are matrix of corresponding active and inactive cables which composed by corresponding columns of matrix $\mathbf{J}(k)$ of state j, respectively. In the same way, $\mathbf{f}_{jA}$ and $\mathbf{f}_{jI}$ are the vectors which composed by corresponding rows of the active and inactive forces of state

j, respectively. Also, $\mathbf{h}(k)$ is defined as follows and its components are named impedance torques:

$$\mathbf{h}(k) = \mathbf{h}'(k) + \mathbf{h}''(k) \tag{28}$$

Step (2): according to practical considerations, among the cases (1) to (4) that one is acceptable which both elements of $\mathbf{f}_{jA}$ will be positive. In order to decrease the number of switching between acceptable mentioned cases during the motion, the desired case is one which has applied in prior step time if as possible. Matrices $\mathbf{J}_{jA}$ and $\mathbf{J}_{jI}$ and vectors $\mathbf{f}_{jA}$ and $\mathbf{f}_{jI}$ related to these cases are shown by $\mathbf{J}_{jA}$ and $\mathbf{J}_{jI}$ and vectors $\mathbf{f}_{lA}$ and $\mathbf{f}_{jI}$, respectively, and l is number of desired case.
Step (3): according to practical considerations (b) to (d), the desired forces of cables are calculated as,

$$\mathbf{f}_{lA,d} = \max(\min(\mathbf{f}_{lA}(k), \mathbf{f}_{\max}, \mathbf{f}_{lA}(k-1) + \Delta\mathbf{f}_{\max}), \mathbf{f}_{\min}, \mathbf{f}_{lA}(k-1) - \Delta\mathbf{f}_{\max}) \tag{29}$$

where,

$$\begin{cases} \mathbf{f}_{\max} = [f_{\max} \quad f_{\max}]^T \\ \mathbf{f}_{\min} = [f_{\min} \quad f_{\min}]^T \\ \Delta\mathbf{f}_{\max} = [\Delta f_{\max} \quad \Delta f_{\max}]^T \end{cases} \tag{30}$$

In Equation (30), $f_{\max}$ and $f_{\min}$ are the maximum and minimum allowable values of cables, respectively. Also, $\Delta f_{\max}$ is the maximum allowable value of variation of the applied forces on the cables at one step time. Hence, the control law can be written as,

$$\begin{cases} \mathbf{f}_A(k) = \max\big(\min\big(\mathbf{J}_{lA}^{-1}(k)\big(\mathbf{h}(k) - \mathbf{J}_{lI}(k)\mathbf{f}_{lI}(k)\big), \mathbf{f}_{\max}, \mathbf{f}_{lA}(k-1) + \Delta\mathbf{f}_{\max}\big) \\ \qquad\qquad , \mathbf{f}_{\min}, \mathbf{f}_{lA}(k-1) - \Delta\mathbf{f}_{\max}) \\ \mathbf{f}_I(k) = \mathbf{f}_{\min} \end{cases} \tag{31}$$

where $\mathbf{f}_A$ and $\mathbf{f}_I$ are the vectors which composed by the corresponding rows of $\mathbf{f}(k)$ that are active and inactive at any time, respectively.
By appropriate select of $\mathbf{M_d}$, $\mathbf{C_d}$ and $\mathbf{K_d}$ according to intended method, control law (31) produces torques that satisfy the corresponding mode requirements.
Finally, the state space of the system can be re-written as Equation (32), and the flowchart of the rehabilitation process is shown in Figure (3).

$$\begin{cases} \boldsymbol{\theta}(k+1) = \boldsymbol{\theta}(k) + T\boldsymbol{\omega}(k) \\ \boldsymbol{\omega}(k+1) = \boldsymbol{\omega}(k) + T\mathbf{M}^{-1}(k)\big(-\mathbf{C}(k)\boldsymbol{\omega}(k) - \mathbf{K}\boldsymbol{\theta}(k) - \mathbf{g}(k) - \boldsymbol{\tau}(k) + \mathbf{B}(k)\mathbf{f}(k)\big) \end{cases} \tag{32}$$

In which, $\boldsymbol{\theta}$ and $\boldsymbol{\omega}$ are the outputs of the system and $\mathbf{f}$ is the input of the system.

5 Simulation and results

The following physical and geometrical parameters of an assumed patient, a descriptive model of the natural resistive torques of the joints and the corresponding estimation parameters, control parameters, simulation parameters, a descriptive model of the predesigned motion, and a descriptive model of the applied torque by the patient in various rehabilitation modes are all necessary for problem simulation.

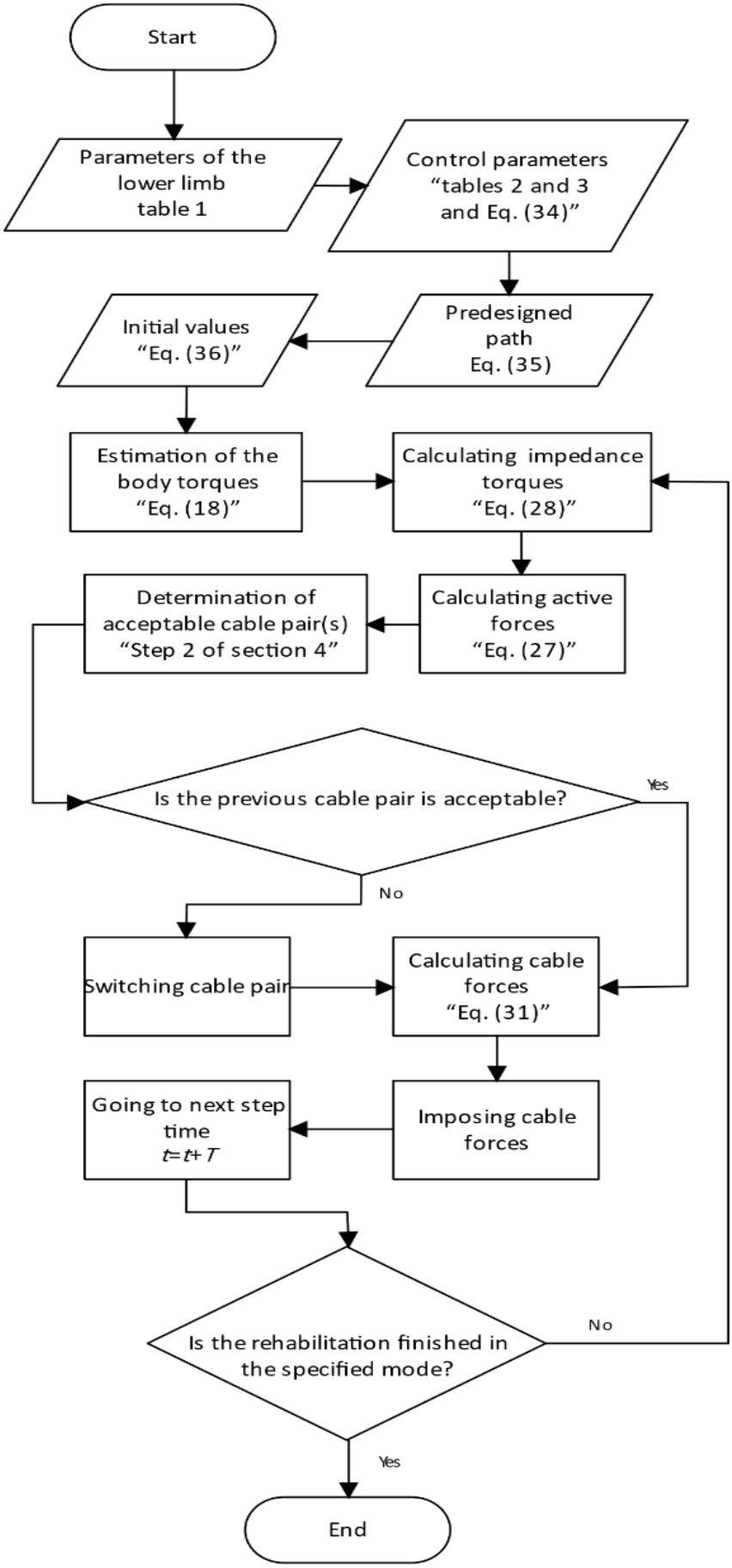

Figure 3 Flowchart of the rehabilitation process

5.1 Simulation data and other information

Physical and geometrical parameters of an assumptive patient are given in Table (1).
The applied torque to each joint due to the body is resultant of the applied torque to the joint from the patient ($\boldsymbol{\tau}_{pj}$) and natural resistive torque of the joint ($\boldsymbol{\tau}_{mj}$). So, we have:

$$\tau_j = \tau_{pj} + \tau_{mj} \qquad j = 1, 2 \tag{33}$$

First term of the above equation is zero in passive mode. Because as mentioned earlier, the patient is unable to apply torque to his/her joints in this mode. According to the nature of physical constraints of the joints and their involved limbs, natural resistive torque of the hip (τ_{m1}) can be considered as resultant of the thigh angle, absolute angle of shank ($\theta_1 + \theta_2$), and their corresponding angular velocity. In such a way, natural resistive torque of the knee (τ_{m2}) can be considered as resultant of the shank angle measured to the hip alignment, absolute angle of the shank ($\theta_1 + \theta_2$), and their corresponding angular velocity (appendix A).
The control parameters include the following three categories:
I) Geometric parameters related to the cables (Table (2))
II) Parameters related to the control constraints and sampling time (Table (3))
III) Coefficients of controller (Equation (34))

Table 1 Physical and geometrical parameters of an assumptive patient [30]

Parameter	Value	Parameter	Value
m_2	3.6 (kg)	m_1	6.8 (kg)
l_2	0.466 (m)	l_1	0.472 (m)
R_2	0.121 (m)	R_1	0.132 (m)
c_2	0.21 (m)	c_1	0.189 (m)
K_2	1 $(N.m)$	K_1	1 $(N.m)$
C_2	0.2 $(N.m.s)$	C_1	0.2 $(N.m.s)$

Table 2 Geometric parameters related to the cables

Parameter	Value (m)	Parameter	Value (m)	Parameter	Value (m)	Parameter	Value (m)
P_{x1}	0.1	P_{x2}	-1	P_{x3}	0.4	P_{x4}	1
P_{y1}	2	P_{y2}	-2	P_{y3}	2	P_{y4}	-2
d_1	0.157	d_2	0.314	d_3	0.155	d_4	0.31
w_1	0.0472	w_2	-0.0472	w_3	0.0466	w_4	-0.0466

Table 3 Parameters related to control constraints and sampling time

Parameter	Value
T	0.01 (sec)
N_d	1
$f_{\max}$	100 (N)
$f_{\min}$	0.1 (N)
$\Delta f_{\max}$	2 (N)

$$\begin{cases} \mathbf{M_d} = \text{diag}([1 \quad 1])(N.m.s^2) \\ \mathbf{C_d} = \text{diag}([12 \quad 12])(N.m.s) \\ \mathbf{K_d} = \text{diag}([25 \quad 25])(N.m) \end{cases} \tag{34}$$

The predesigned path for control implementation is descripted in the following equations in terms of radian:

$$\begin{cases} \theta_{1d} = -\dfrac{\pi}{6}(1 - \cos \pi t) \\ \theta_{2d} = \dfrac{\pi}{8}(1 - \cos \pi t) \end{cases} \tag{35}$$

Finally, Simulation is implemented within 20 seconds and step time 20 milliseconds with the following initial values:

$$\begin{cases} \boldsymbol{\theta} = [0 \quad 0]\ (deg) \\ \dot{\boldsymbol{\theta}} = [0 \quad 0]\ (deg/sec) \\ \boldsymbol{\tau_p} = [\tau_{p1} \quad \tau_{p2}] = [0 \quad 0]\ (N.m) \\ \mathbf{f} = [0.1 \quad 0.1 \quad 0.1 \quad 0.1]\ (N) \end{cases} \tag{36}$$

And the simulation is done using a computer with 11th Gen Intel(R) Core(TM) i5-11400H @ 2.70GHz Processor, Win 11 and 16.0 GB DDR4 RAM.

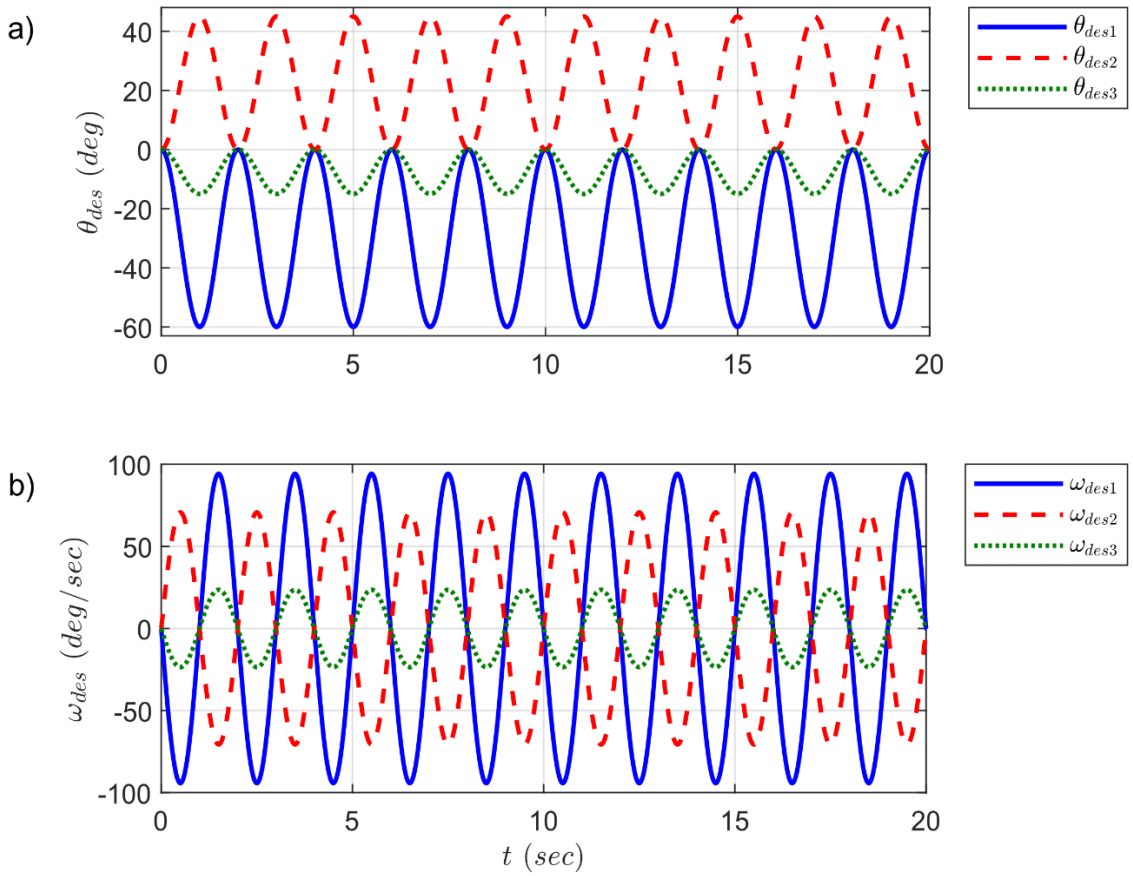

Figure 4 a) Desired angles in both modes, **b**) desired angular velocity in both modes: thigh angle (solid line), shank angle relative to the thigh (dashed line), absolute shank angle (dotted line)

So, the predesigned angles and the corresponding angular velocities are considered as desired angles and angular velocities, respectively which shown in Fig. (4) for 10 cycles of motion.
As was already stated, the patient can only apply a small portion of the required torques in the active-assistive mode in order to follow the predesigned route; the cables fill in the remaining torque gaps.
Now, the torques that patient applies at each two rehabilitation modes are descripted. In the passive mode, the patient is passive practically, and the both applied torques by patient are zero. So, the torques that needed to track the predesigned path are applied by actuators.
As was already stated, the patient's ability has somewhat returned when in assistive mode. Thus, in this mode, the actuators assist the patient in performing action that has been predetermined. In this mode, it is presumable that the patient exerts a varying amount of torque, which is applied by the actuators in the passive mode, and that the actuators make up for any leftover required value. It is noteworthy that the patient's capacity for recovery grows. The previously stated fraction's upper and lower bounds grow. As a result, the patient's imposed torque is described by a fraction between 0.2 and 0.6 (appendix B).

5.2 Results

In this section, the results of simulation and cable robot control are shown in two separate subsections and the analysis related to each other will be expressed.

5.2.1 Results of rehabilitation in Passive mode

Figures (5) and (6) represent the designed control algorithm can steer the hip and the knee angles to follow the corresponding desired values.

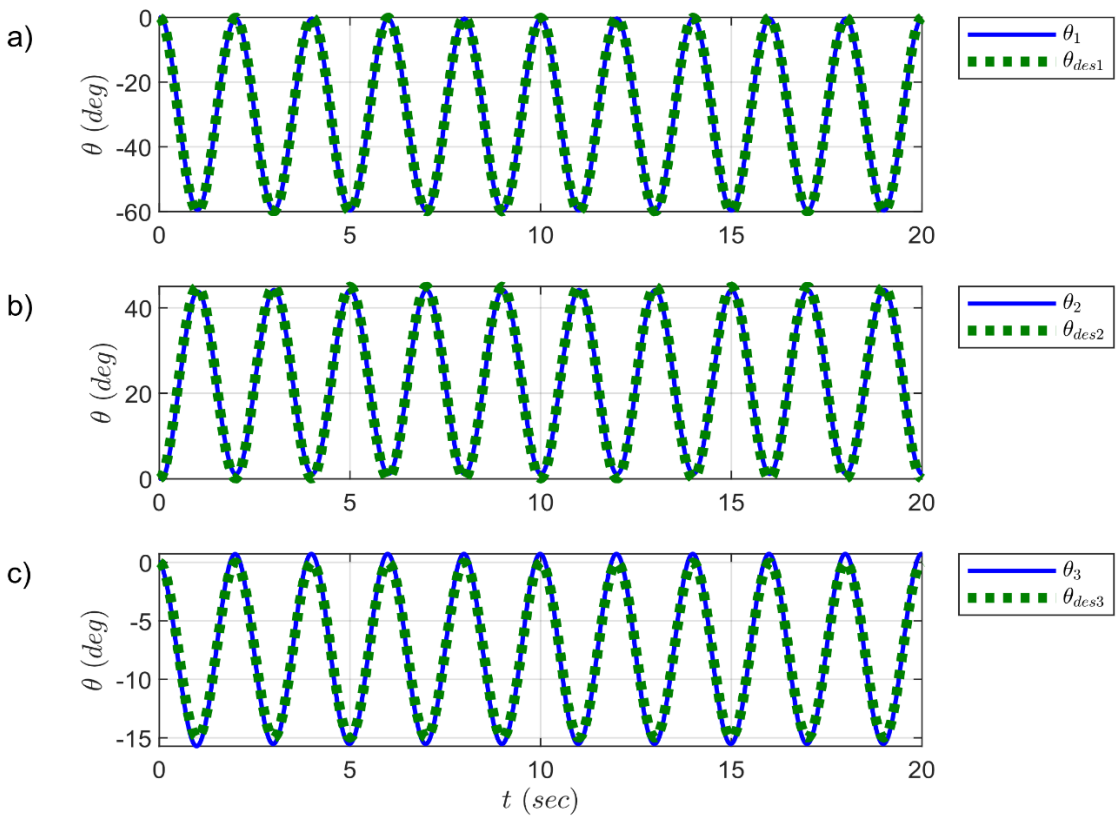

Figure 5 a) thigh angle in the passive mode, **b**) shank angle relative to the thigh in the passive mode, **c**) absolute shank angle in the passive mode: angle (solid line), desired angle (dotted line)

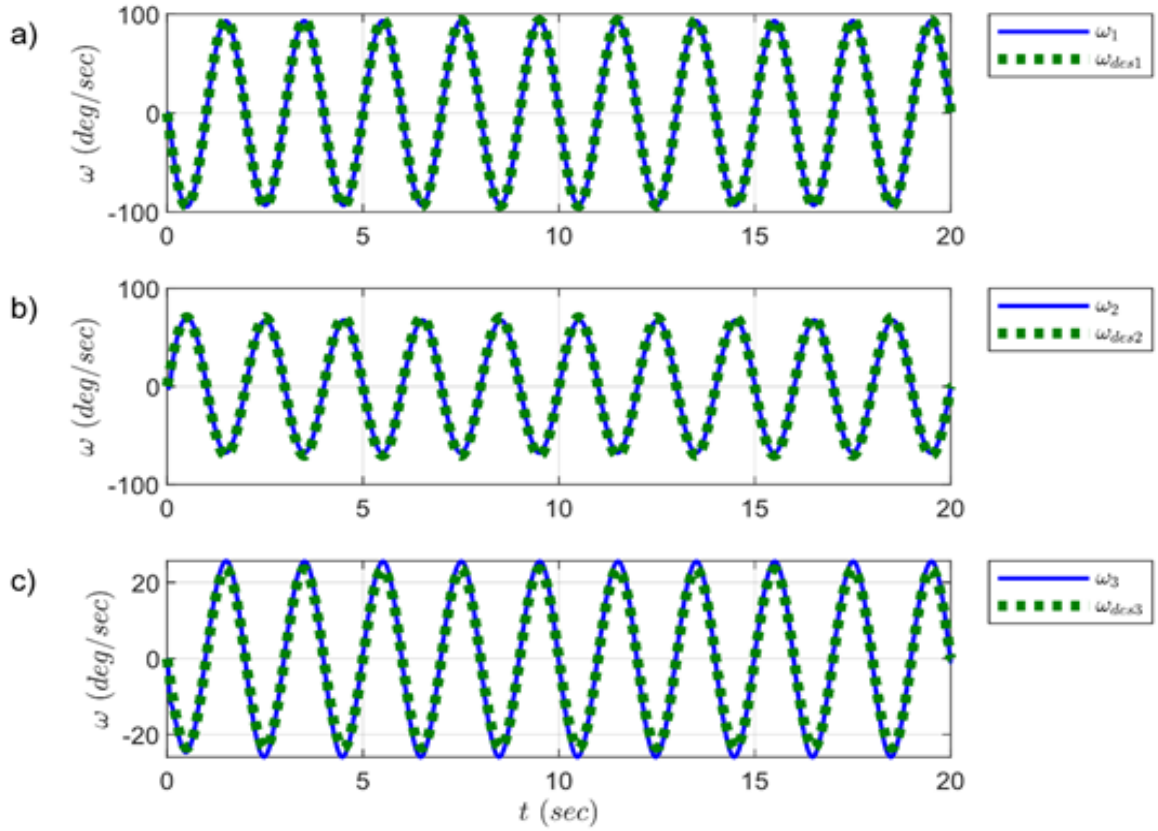

Figure 6 a) thigh angle in the passive mode, **b**) shank angle relative to the thigh in the passive mode, **c**) absolute shank angle in the passive mode: angular velocity (solid line), desired angular velocity (dotted line)

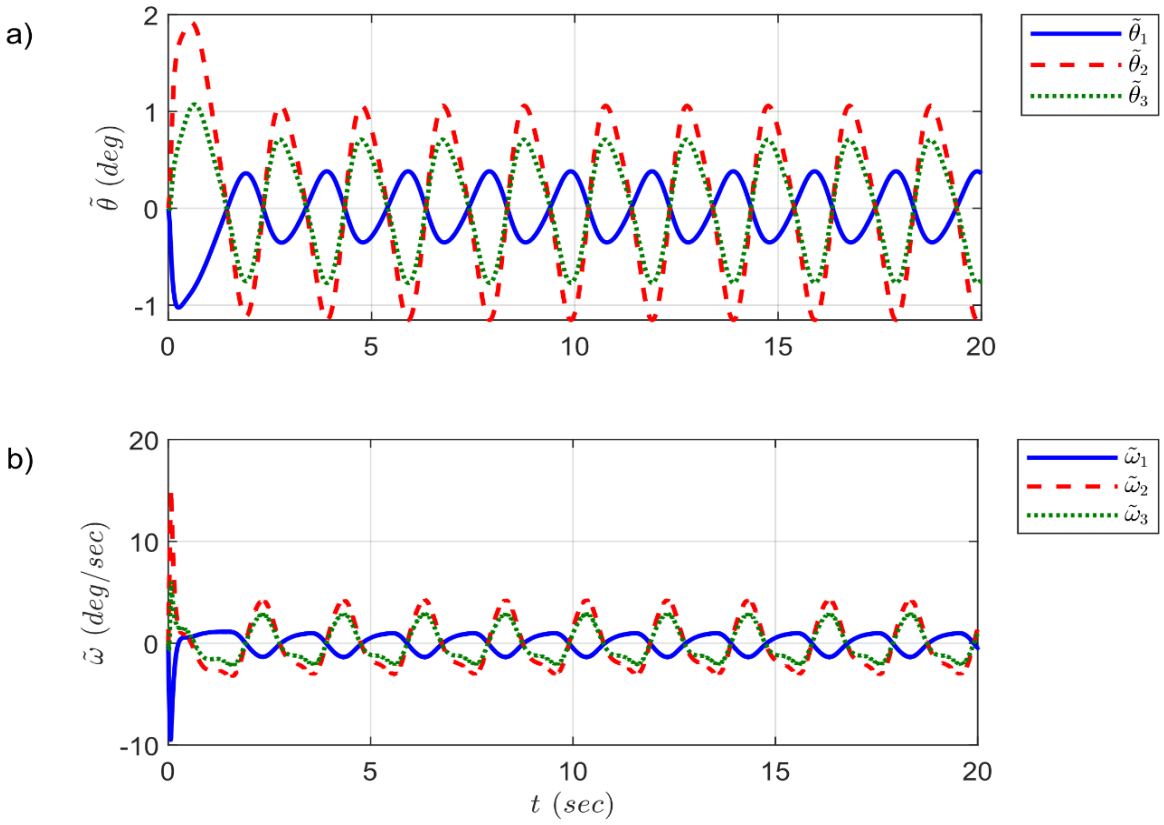

Figure 7 a) error of angles in the passive mode, **b**) error of angular velocities in the passive mode: thigh angle (solid line), shank angle relative to the thigh (dashed line), absolute shank angle (dotted line)

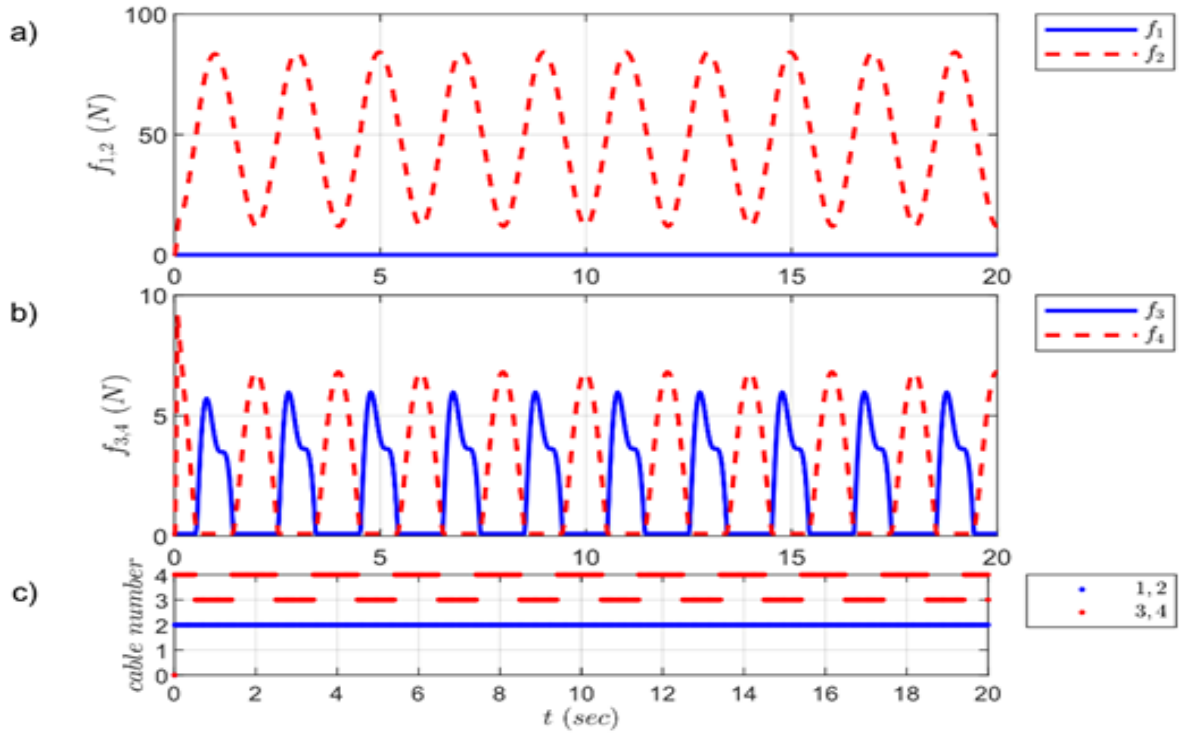

Figure 8 a) applied forces to the cables (1) and (2) in the passive mode, **b**) applied forces to the cables (3) and (4) in the passive mode: cables (1) and (3) (solid line), cables (2) and (4) (dashed line), **c**) cable number

On the other hand, in case of steady-state response, tracking of the predesigned motion has been preserved with proper accuracy. The value of tracking error in the angle of thigh, shank angle related to thigh and absolute angle of shank is 0.3, 1.05 and 0.7 degrees, respectively. Also, as shown in Figure (7), the values of the mentioned error in the relative angular velocity of the thigh, angular velocity of the shank related to the thigh and absolute angular velocity of the shank is 1.5, 5 and 4.6 rad/sec. Transient state error has been ignored and the maximum error of afterward mentioned. The applied forces to the cables are depicted in Figure (8). As seen in Figure (8), during the pre-designed motion in the passive mode, no force is imparted to cable (1). Actually, cable (1) pulls the leg down can be used to justify this. Since the weight of the leg can move the body on its own during thigh down movement, no effort is necessary. The force of cable (3) is not zero in the case of the shank because of the form of the specified intended output and the dependence of the shank angle to the leg. In this case, the controller works correctly and applies the appropriate force to perform the predesigned motion. Also, the run time of this mode is 0.141 second which is acceptable considering the total simulation time and it is guaranteed that the system works at real time.

5.2.2 Results of rehabilitation in active-assistive mode

As mentioned earlier, it is needed that the actuator help the patient to move the knee and the hip joints perfectly. Figures (9) and (10) show that the angles and the angular velocities of the joints follow the corresponding desired motion. It can be seen that the designed control algorithm has been able to steer the hip and the knee to follow the corresponding desired angles in a very short time. On the other hand, in case of steady-state response, tracking of the desired outputs is preserved properly and appropriate accuracy has achieved.
Here, tracking error in the thigh angle, the shank angle related to the thigh and absolute shank angle are 0.27, 0.45 and 0.15 degrees, respectively. Also, as shown in Figure (11), the error of the angular velocities of the thigh, the shank related to thigh and absolute angular velocity of the shank are 1.1, 2.4 and 2.2 rad/sec, respectively.

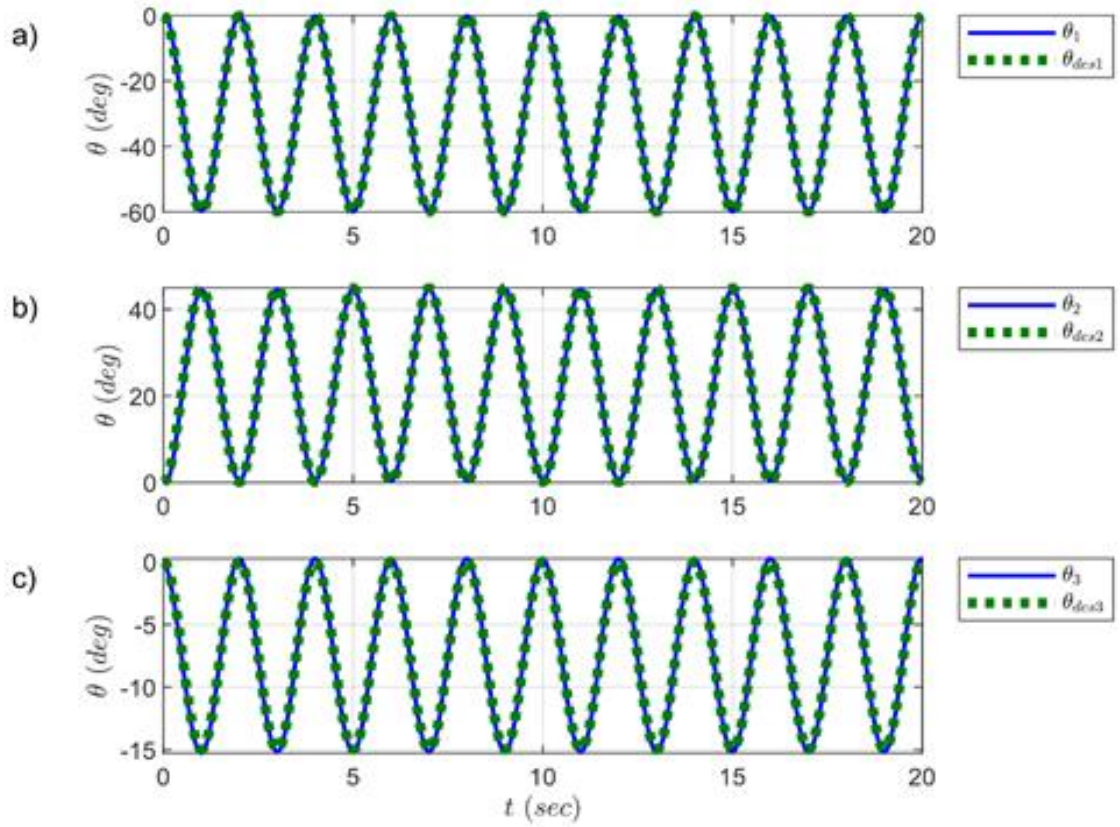

Figure 9 a) thigh angle in the active-assistive mode, **b**) shank angle relative to the thigh in the active-assistive mode, **c**) absolute shank angle in the active-assistive mode: angle (solid line), desired angle (dotted line)

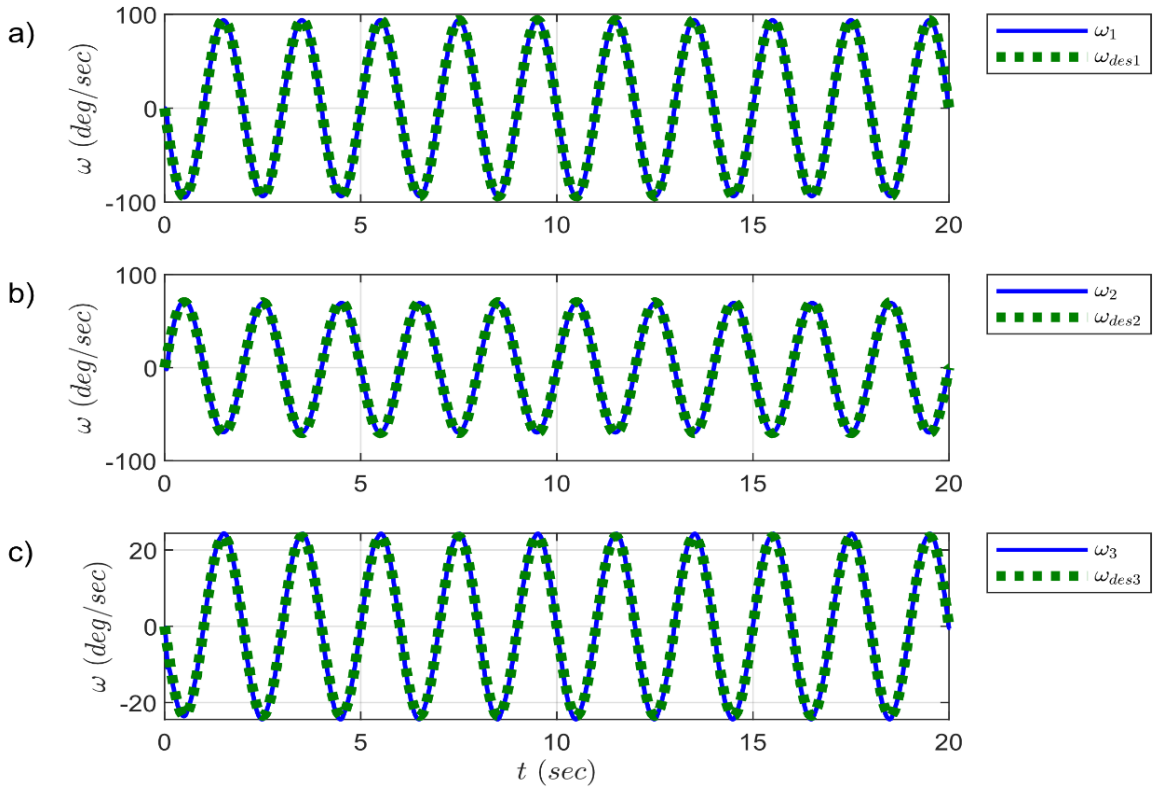

Figure 10 a) thigh angle in the active-assistive mode, **b**) shank angle relative to the thigh in the active-assistive mode, **c**) absolute shank angle in the active-assistive mode: angular velocity (solid line), desired angular velocity (dotted line)

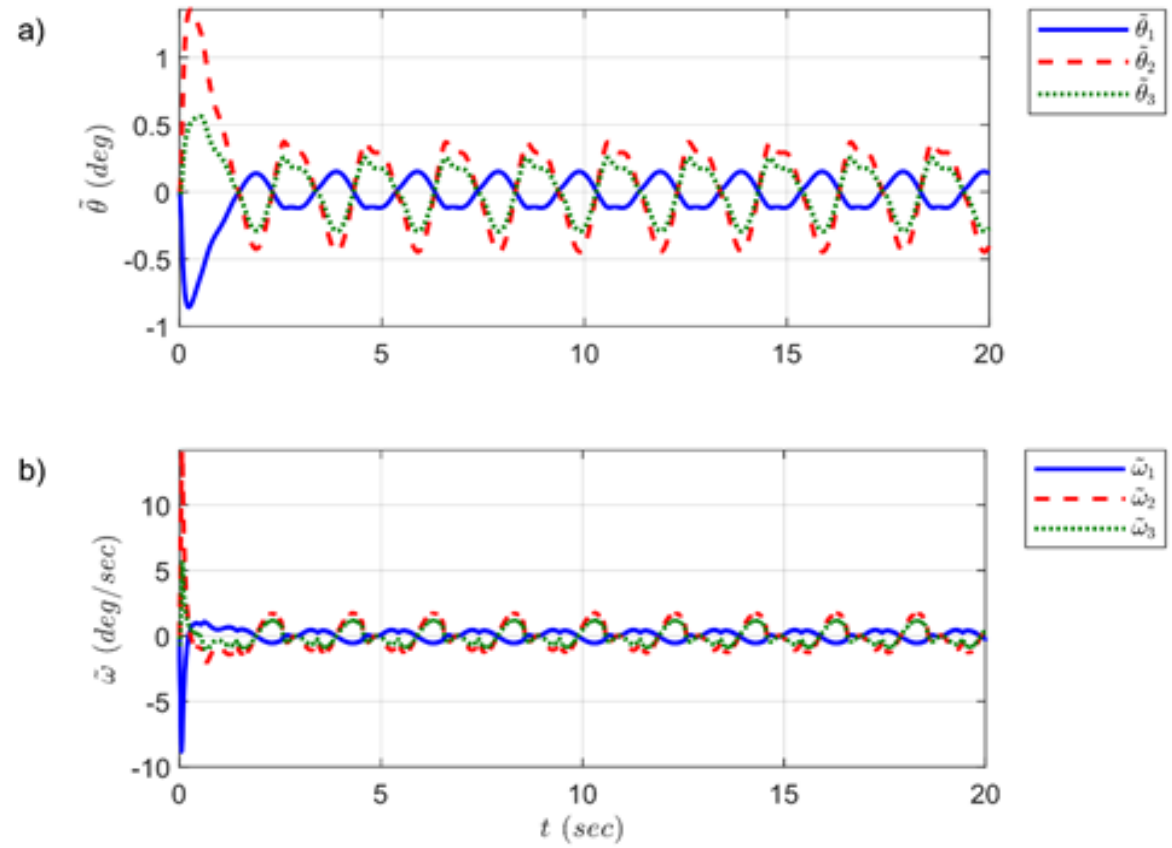

Figure 11 a) error of angles in the active-assistive mode, **b**) error of angular velocities in the active-assistive mode: thigh angle (solid line), shank angle relative to the thigh (dashed line), absolute shank angle (dotted line)

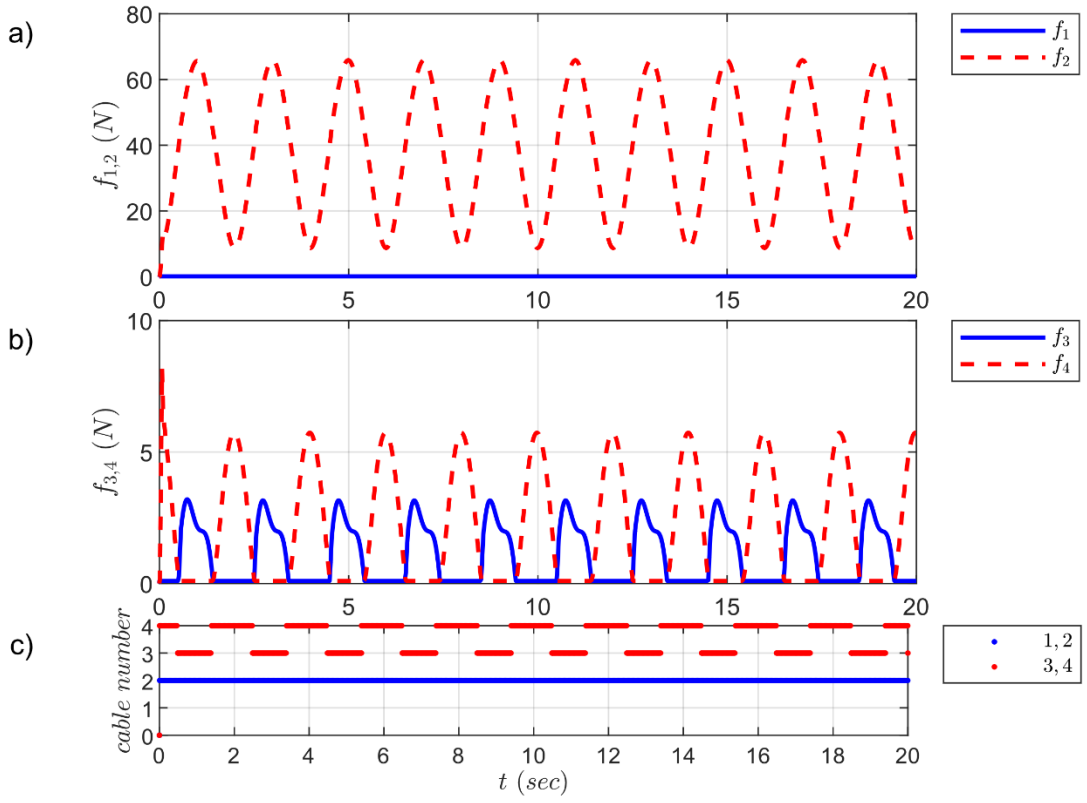

Figure 12 a) applied forces to the cables (1) and (2) in the active-assistive mode, **b**) applied forces to the cables (3) and (4) in the active-assistive mode: cables (1) and (3) (solid line), cables (2) and (4) (dashed line), c) cable number

The transient state error is neglected in this case. No force is imparted to cable (1), as seen in Figure (12). Since the patient is trying to apply the necessary torques to their joints in order to perform the desired motion in this mode, the values of the applied torques to the patient joints and values of the forces have decreased. This is evident from what has been said about how to simulate the inputs in this mode and from comparing Figure (12) with (8).
The control system during the motion, helps the thigh to move. This is %97.984 for the shank which is very acceptable. Also, run time is 0.097 seconds in this mode which is short considering the total simulation time of 20 seconds, and it is guaranteed that the control system is real-time.

6 Conclusion

The paper has focused on examining the simulation and control of a 2-DOF cable robot with four cables in the sagittal plane. The dynamic equations of motion of the limbs have been derived using Lagrange's approach. To account for the inherent stiffness of lower limbs, a model was created for natural resistive torques. The control algorithm was developed using impedance control approach to regulate torques and angular positions. Practical restrictions such as cable pretensions and maximal capacities were taken into account, as well. The concept involves using one opposing cable for each limb and another under minimal tension to provide ease during rehabilitation. This can also help patients concentrate on their recovery activities.
It has been revealed that the control commands are effective in delivering the necessary forces to generate the required torques for directing predesigned motions in both modes of rehabilitation. The short transient period is ideal for rehabilitation purposes, and the commands have been generated in real-time while meeting control constraints. This approach can be utilized for the active-resistive mode of rehabilitation to enhance muscle strength. Moreover, adjusting the attached points of the cables to be perpendicular to the involved limbs can help achieve a more near-optimal control effort.

References

[1] C. H. Guzmán, A. Blanco, J. A. Brizuela, and F. A. Gómez, "Robust Control of a Hip–joint Rehabilitation Robot," *Biomedical Signal Processing and Control*, Vol. 35, pp. 100-109, 2017, doi: https://doi.org/10.1016/j.bspc.2017.03.002.

[2] G. Rosati, S. Masiero, and A. Rossi, "On the Use of Cable-driven Robots in Early Inpatient Stroke Rehabilitation," in *Advances in Italian Mechanism Science: Proceedings of the First International Conference of IFToMM Italy*, 2017: Springer, Cham, pp. 551-558, doi: https://doi.org/10.1007/978-3-319-48375-7_59.

[3] D. Zanotto, G. Rosati, S. Minto, and A. Rossi, "Sophia-3: A Semiadaptive Cable-driven Rehabilitation Device with a Tilting Working Plane," *IEEE Transactions on Robotics*, Vol. 30, No. 4, pp. 974-979, 2014, doi: https://doi.org/10.1109/TRO.2014.2301532.

[4] M. Wu, T. G. Hornby, J. M. Landry, H. Roth, and B. D. Schmit, "A Cable-driven Locomotor Training System for Restoration of Gait in Human SCI," *Gait & posture*, Vol. 33, No. 2, pp. 256-260, 2011, doi: https://doi.org/10.1016/j.gaitpost.2010.11.016.

[5] P. K. Jamwal, S. Hussain, Y. H. Tsoi, M. H. Ghayesh, and S. Q. Xie, "Musculoskeletal Modelling of Human Ankle Complex: Estimation of Ankle Joint Moments," *Clinical Biomechanics*, Vol. 44, pp. 75-82, 2017, doi: https://doi.org/10.1016/j.clinbiomech.2017.03.010.

[6] G. Abbasnejad, J. Yoon, and H. Lee, "Optimum Kinematic Design of a Planar Cable-driven Parallel Robot with Wrench-closure Gait Trajectory," *Mechanism and Machine Theory*, Vol. 99, pp. 1-18, 2016, doi: https://doi.org/10.1016/j.mechmachtheory.2015.12.009.

[7] Q. Duan, V. Vashista, and S. K. Agrawal, "Effect on Wrench-feasible Workspace of Cable-driven Parallel Robots by Adding Springs," *Mechanism and Machine Theory*, Vol. 86, pp. 201-210, 2015, doi: https://doi.org/10.1016/j.mechmachtheory.2014.12.009.

[8] B. M. Fard, T. Padargani, and S. Saki, "Optimum Determination of Motor Mount Locations for a Cable-driven Rehabilitation Robot," in *2014 Second RSI/ISM International Conference on Robotics and Mechatronics (ICRoM)*, 2014: IEEE, Tehran, Iran, pp. 864-869, doi: https://doi.org/10.1109/ICRoM.2014.6991013.

[9] M. Bolliger, R. Banz, V. Dietz, and L. Lünenburger, "Standardized Voluntary Force Measurement in a Lower Extremity Rehabilitation Robot," *Journal of Neuroengineering and Rehabilitation*, Vol. 5, pp. 1-8, 2008, doi: https://doi.org/10.1186/1743-0003-5-23.

[10] T. Eiammanussakul and V. Sangveraphunsiri, "A Lower Limb Rehabilitation Robot in Sitting Position with a Review of Training Activities," *Journal of Healthcare Engineering*, Vol. 2018, 2018, doi: https://doi.org/10.1155/2018/1927807.

[11] M. Bianchi, F. Fanelli, E. Meli, A. Ridolfi, F. Vannetti, M. Bianchini, and B. Allotta "Optimization-based Scaling Procedure for the Design of Fully Portable Hand Exoskeletons," *Meccanica*, Vol. 53, pp. 3157-3175, 2018, doi: https://doi.org/10.1007/s11012-018-0858-7.

[12] B. Ugurlu, M. Nishimura, K. Hyodo, M. Kawanishi, and T. Narikiyo, "Proof of Concept for Robot-aided Upper Limb Rehabilitation using Disturbance Observers," *IEEE Transactions on Human-Machine Systems*, Vol. 45, No. 1, pp. 110-118, 2014, doi: https://doi.org/10.1109/THMS.2014.2362816.

[13] J. A. Saglia, N. G. Tsagarakis, J. S. Dai, and D. G. Caldwell, "Control Strategies for Patient-assisted Training using the Ankle Rehabilitation Robot (ARBOT)," *IEEE/ASME Transactions on Mechatronics*, Vol. 18, No. 6, pp. 1799-1808, 2012, doi: https://doi.org/10.1109/TMECH.2012.2214228.

[14] A. L. Jutinico, J. C. Jaimes, F. M. Escalante, J. C. Perez-Ibarra, M. H. Terra, and A. A. Siqueira, "Impedance Control for Robotic Rehabilitation: a Robust Markovian Approach," *Frontiers in Neurorobotics*, Vol. 11, p. 43, 2017, doi: https://doi.org/10.3389/fnbot.2017.00043.

[15] E. L. Oyman, M. Y. Korkut, C. Ylmaz, Z. Y. Bayraktaroglu, and M. S. Arslan, "Design and Control of a Cable-driven Rehabilitation Robot for Upper and Lower Limbs," *Robotica*, Vol. 40, No. 1, pp. 1-37, 2022, doi: https://doi.org/10.1017/S0263574721000357.

[16] B. Brahmi, M. Driscoll, I. K. El Bojairami, M. Saad, and A. Brahmi, "Novel Adaptive Impedance Control for Exoskeleton Robot for Rehabilitation using a Nonlinear Time-delay Disturbance Observer," *ISA Transactions*, Vol. 108, pp. 381-392, 2021, doi: https://doi.org/10.1016/j.isatra.2020.08.036.

[17] Z. Chen, Q. Guo, H. Xiong, D. Jiang, and Y. Yan, "Control and Implementation of 2-DOF Lower Limb Exoskeleton Experiment Platform," *Chinese Journal of Mechanical Engineering*, Vol. 34, No. 1, pp. 1-17, 2021, doi: https://doi.org/10.1186/s10033-021-00537-8.

[18] L. Luo, M.J. Foo, M. Ramanathan, J.K. Er, C. H. Chiam, L. Li, W. Y. Yau and W. T. Ang, "Trajectory Generation and Control of a Lower Limb Exoskeleton for Gait Assistance," *Journal of Intelligent & Robotic Systems*, Vol. 106, No. 3, p. 64, 2022, doi: https://doi.org/10.1007/s10846-022-01763-5.

[19] N. S. Seyfi and A. K. Khalaji, "Robust Control of a Cable-driven Rehabilitation Robot for Lower and Upper Limbs," *ISA Transactions*, Vol. 125, pp. 268-289, 2022, doi: https://doi.org/10.1016/j.isatra.2021.07.016.

[20] Z. Xu and L. Xie, "Cable-driven Flexible Exoskeleton Robot for Abnormal Gait Rehabilitation," *Journal of Shanghai Jiaotong University (Science)*, Vol. 27, No. 2, pp. 231-239, 2022, doi: https://doi.org/10.1007/s12204-021-2403-4.

[21] Y. Zhang, T. Li, H. Tao, F. Liu, B. Hu, M. Wu, and H. Yu," Research on Adaptive Impedance Control Technology of Upper Limb Rehabilitation Robot Based on Impedance Parameter Prediction," *Frontiers in Bioengineering and Biotechnology*, Vol. 11, 2023, doi: https://doi.org/10.3389/fbioe.2023.1332689.

[22] Y. Wang, L. Wang, K. Wang, Z. Mo, J. Li, and L. Yi, "Research on a New Cable-driven Lower Limb Rehabilitation Robot with Bilateral Coordination Control," *Proceedings of the Institution of Mechanical Engineers, Part C: Journal of Mechanical Engineering Science*, p. 09544062231223873, 2024, doi: https://doi.org/10.1177/09544062231223873.

[23] R. Tang, Q. Yang, and R. Song, "Variable Impedance Control Based on Target Position and Tracking Error for Rehabilitation Robots During a Reaching Task," *Frontiers in Neurorobotics*, Vol. 16, p. 850692, 2022, doi: https://doi.org/10.3389/fnbot.2022.850692.

[24] K. Maqsood, J. Xia, D. Huang, and Y. Li, "Robot Assisted Training for Upper Limbs using Impedance Control Based on Iterative Learning," in *2021 33rd Chinese Control and Decision Conference (CCDC)*, 2021: IEEE, Kunming, China, pp. 743-748, doi: https://doi.org/10.1109/CCDC52312.2021.9601842.

[25] H. De las Casas, S. Bianco, and H. Richter, "Targeted Muscle Effort Distribution with Exercise Robots: Trajectory and Resistance Effects," *Medical Engineering & Physics*, Vol. 94, pp. 70-79, 2021, doi: https://doi.org/10.1016/j.medengphy.2021.06.008.

[26] P. K. Jamwal, S. Hussain, M. H. Ghayesh, and S. V. Rogozina, "Adaptive Impedance Control of Parallel Ankle Rehabilitation Robot," *Journal of Dynamic Systems, Measurement, and Control*, Vol. 139, No. 11, p. 111006, 2017, doi: https://doi.org/10.1115/1.4036560.

[27] M. Mokhtari, M. Taghizadeh, and M. Mazare, "Impedance Control Based on Optimal Adaptive High Order Super Twisting Sliding Mode for a 7-DOF Lower Limb Exoskeleton," *Meccanica*, Vol. 56, pp. 535-548, 2021, doi: https://doi.org/10.1007/s11012-021-01308-4.

[28] N. Kieuvongngam, A. Sutapun, and V. Sangeveraphunsiri, "Novel Design and Implementation of a Knee Exoskeleton for Gait Rehabilitation with Impedance Control

Strategy," *Engineering Journal*, Vol. 26, No. 11, pp. 13-27, 2022, doi: https://doi.org/10.4186/ej.2022.26.11.13.

[29] A. M. Dietrich, "Whole-body Impedance Control of Wheeled Humanoid Robots," Technische Universität München, 2015, [Online], Available: https://doi.org/10.1007/978-3-319-40557-5.

[30] A. Alamdari, "Cable-driven Articulated Rehabilitation System for Gait Training," PhD Thesis, Department of Mechanical and Aerospace Engineering, State University of New York at Buffalo, 2016, [Online], Available: https://www.proquest.com/openview/809bbdc7ad4d95ba46643d031014815c/1?pq-origsite=gscholar&cbl=18750.

Nomenclature

English Symbols

C	Torsional damper constant
K	Linear spring stiffness
m	Mass
R_i	Gyration radius
T	Sampling time

Greek symbols

δW	Virtual work
θ_i	Generalized coordinates.
$\dot{\theta}$	Angular velocity
$\ddot{\theta}$	Angular acceleration
$\boldsymbol{\tau}$	Torque
$\hat{\boldsymbol{\tau}}$	Estimated values of torque
ω	Angular velocity

Appendix A

In order to estimation of natural resistive torques of the hip and knee (τ_{m1} and τ_{m2}), some recorded values such as θ_1, θ_2, $\dot{\theta}_1$ and $\dot{\theta}_2$ are considered as independent variables. In the other hand, τ_{m1} and τ_{m2} are considered as dependent variables. So, using regression methods two four-variable functions are approximated. We must presume that the functions have the specified forms in order to simulate. The relationships between the torques and independent variables are explained qualitatively in this manner, in accordance with some physical ideas. In the reality, the patient feels these torques as discomfort in the associated joints. Pain is experienced during some range of motion in the patient's extremities because of the structure of the joints. Pain threshold angles are the angles at which pain starts to increase with further movement in the same direction as the pain is already increasing. The lower limit of the thigh pain threshold angle, the shank pain threshold angle relative to the thigh, and the absolute shank pain threshold angle are denoted by θ_{L1}, θ_{L2} and θ_{L3}, respectively. Similarly, the upper limit of these angles at the pain threshold angle is denoted by θ_{H1}, θ_{H2} and θ_{H3}, respectively. On the other hand, the thigh and the shank have a limited range of motion.

The lower limit of the thigh angle, the angl e of the shank relative to the thigh, and the absolute angle of the shank are denoted by $\theta_{\min 1}$, $\theta_{\min 2}$ and $\theta_{\min 3}$, respectively. Similarly, the upper limit of these angles are denoted by $\theta_{\max 1}$, $\theta_{\max 2}$ and $\theta_{\max 3}$, respectively.
The passage of the thigh angle and the angle of the shank relative to the thigh from the pain threshold angle leads to an increase in torsional stiffness in the hip and the knee joints, respectively. The values of this torsional stiffness at the lower threshold of the pain threshold angle are indicated by K_{pL1} and K_{pL2} for the hip and knee joints, respectively. Similarly, the values of these torsional stiffness at the upper threshold of the pain threshold angle are denoted by K_{pH1} and K_{pH2}. But, passing the angle of the shank from the pain threshold angle leads to an increase in torsional stiffness in the both joints. The values of these torsional stiffness at the lower threshold of the pain threshold angles are indicated by K_{sL1} and K_{sL2} for the hip and knee joints, respectively. Similarly, the values of these torsional stiffness at the upper threshold of the pain threshold angle are denoted by K_{sH1} and K_{sH2}.
According to the above definition for the values of torsional damping corresponding to torsional stiffness are denoted by C_{pL1}, C_{pH1}, C_{pL2}, C_{pH2}, C_{pL1}, C_{sL2}, $C_{sH1}$and C_{pH2}. Therefore, τ_{m1} and τ_{m2} are defined as:

$$\begin{cases}\tau_{m1} = (\theta_1, \theta_2, \dot{\theta}_1, \dot{\theta}_2) = \varphi_{1,1}(\theta_1) + \varphi_{1,2}(\theta_3) - \varphi_{1,3}(\theta_1)\dot{\theta}_1 - \varphi_{1,4}(\theta_3)\dot{\theta}_3 \\ \tau_{m2} = (\theta_1, \theta_2, \dot{\theta}_1, \dot{\theta}_2) = \varphi_{2,1}(\theta_2) + \varphi_{2,2}(\theta_3) - \varphi_{2,3}(\theta_2)\dot{\theta}_2 - \varphi_{2,4}(\theta_3)\dot{\theta}_3 \end{cases} \quad \text{(A-1)}$$

In which $\theta_3 = \theta_1 + \theta_2$, and

$$\varphi_{j,1} = \begin{cases} -K_{pLj}\exp\left(a_{pLj}\left(\frac{\theta_j - \theta_{Lj}}{\theta_{\min j} - \theta_{Lj}}\right)^2\right)(\theta_j - \theta_{Lj}) & \theta_j < \theta_{Lj} \\ -K_{pHj}\exp\left(a_{pHj}\left(\frac{\theta_j - \theta_{Hj}}{\theta_{\max j} - \theta_{Hj}}\right)^2\right)(\theta_j - \theta_{Hj}) & \theta_j < \theta_j \end{cases} \quad j = 1,2 \quad \text{(A-2)}$$

$$\varphi_{j,2} = \begin{cases} -K_{sLj}\exp\left(a_{sLj}\left(\frac{\theta_3 - \theta_{L3}}{\theta_{\min 3} - \theta_{L3}}\right)^2\right)(\theta_3 - \theta_{L3}) & \theta_3 < \theta_{L3} \\ -K_{sHj}\exp\left(a_{sHj}\left(\frac{\theta_3 - \theta_{H3}}{\theta_{\max j} - \theta_{Hj}}\right)^2\right)(\theta_3 - \theta_{H3}) & \theta_3 < \theta_3 \end{cases} \quad j = 1,2 \quad \text{(A-3)}$$

$$\varphi_{j,3} = \begin{cases} -C_{pLj}\exp\left(a_{pLj}\left(\frac{\theta_j - \theta_{Lj}}{\theta_{\min j} - \theta_{Lj}}\right)^2\right)(\theta_j - \theta_{Lj}) & \theta_j < \theta_{Lj} \\ -C_{pHj}\exp\left(a_{pHj}\left(\frac{\theta_j - \theta_{Hj}}{\theta_{\max j} - \theta_{Hj}}\right)^2\right)(\theta_j - \theta_{Hj}) & \theta_j < \theta_j \end{cases} \quad j = 1,2 \quad \text{(A-4)}$$

$$\varphi_{j,4} = \begin{cases} -C_{sLj}\exp\left(a_{sLj}\left(\frac{\theta_3 - \theta_{L3}}{\theta_{\min 3} - \theta_{L3}}\right)^2\right)(\theta_3 - \theta_{L3}) & \theta_3 < \theta_{L3} \\ -C_{sHj}\exp\left(a_{sHj}\left(\frac{\theta_3 - \theta_{H3}}{\theta_{\max j} - \theta_{Hj}}\right)^2\right)(\theta_3 - \theta_{H3}) & \theta_3 < \theta_3 \end{cases} \quad j = 1,2 \quad \text{(A-5)}$$

$$\varphi_{j,1}, \varphi_{j,2}, \varphi_{j,3}, \varphi_{j,4} = 0 \quad otherwise \quad j = 1,2 \quad \text{(A-6)}$$

Table A-1 The values of the torsional stiffnesses and damping at the thresholds of the angles of hip and knee and other coefficients to describe the natural resistive torques of the joints

Parameter	Value ($N.m$)	Parameter	Value ($N.m.s$)	Parameter	Value
K_{pL1}	10^{-3}	C_{pL1}	10^{-3}	a_{pL1}	4
K_{pL2}	10^{-2}	C_{pL2}	10^{-2}	a_{pL2}	4.5
K_{pH1}	10^{-3}	C_{pH1}	10^{-3}	a_{pH1}	4
K_{pH2}	10^{-2}	C_{pH2}	10^{-2}	a_{pH2}	4.5
K_{sL1}	10^{-3}	C_{sL1}	10^{-3}	a_{sL1}	4
K_{sL2}	10^{-3}	C_{sL2}	10^{-3}	a_{sL2}	4
K_{sL1}	10^{-3}	C_{sL1}	10^{-3}	a_{sL1}	4
K_{sL2}	10^{-3}	C_{sL2}	10^{-3}	a_{sL2}	4

Table A-2 The values of thresholds of the angles of hip and knee

Parameter	Value (deg)	Parameter	Value (deg)	Parameter	Value (deg)
θ_{min1}	-90	θ_{min2}	-5	θ_{min3}	-60
θ_{L1}	-80	θ_{L2}	0	θ_{L3}	-45
θ_{H1}	10	θ_{H2}	110	θ_{H3}	100
θ_{max1}	20	θ_{max2}	120	θ_{max3}	120

In which the values of corresponding parameters in the right hands of the above equations are listed in Table (A-1), and the values of thresholds of the angles of hip and knee are listed in Table (A-2).
Since error is unavoidable in estimating of natural resistive torques of the joints, the values of these torques are estimated with 5% tolerance of values of estimations of (A-1).

Appendix B

In order to determine the patient's imposed torques, the cables forces must be measured in the passive mode, earlier. So, the applied torque vector which are produced by these forces is obtained as:

$$\boldsymbol{\tau}_d(k) = [\tau_{1d}(k) \quad \tau_{2d}(k)]^T = \mathbf{Bf} \tag{B-1}$$

Afterward, a random number between 0 and 1 is selected and shown by R. After more, $\tau^*_{\max}$ and $\tau^*_{\min}$ are upper and lower of earlier mentioned fraction, respectively, and $\tau''_j(k)$ are define as following:

$$\begin{cases} \tau^*_{\max} = 0.6 \\ \tau^*_{\min} = 0.2 \\ \tau''_j(k) = \tau_{pj}(k-1) \qquad\qquad j = 1, 2 \\ +\min\left(\left[\left(\max\left[-T\dot{\tau}_{pj\max} \quad \left((\tau^*_{\max} - \tau^*_{\min})R + \tau^*_{\max}\right)\left(\tau_{jd}(k) - \tau_{jd}(k-1)\right)\right]\right) \\ T\dot{\tau}_{pj\max}\right]\right) \end{cases} \tag{B-2}$$

$\dot{\tau}_{pj\max}$ is the maximum rate of torque variation applied by the patient. This parameter explains the maximum power of the patient for changing the torque applied by the patient.

$$\dot{\tau}_{p1\max} = 800; \quad \dot{\tau}_{p2\max} = 500 \tag{B-3}$$

Then, the applied torque by the patient is obtained as following:

$$\tau_{pj}(k) = \begin{cases} \min\left(\left[\max\left(\left[\tau^*_{\min}\tau_{jd}(k) \quad \tau''_j(k)\right]\right) \quad \tau^*_{\max}\tau_{jd}(k)\right]\right) & \tau_{jd}(k) > 0 \\ \min\left(\left[\max\left(\left[\tau^*_{\max}\tau_{jd}(k) \quad \tau''_j(k)\right]\right) \quad \tau^*_{\min}\tau_{jd}(k)\right]\right) & \tau_{jd}(k) < 0 \quad j = 1,2 \\ 0 & \tau_{jd}(k) = 0 \end{cases} \tag{B-4}$$